

# Systemic exposure to bacterial amyloid curli alters the gut mucosal immune response and the microbiome, exacerbating *Salmonella*-induced arthritis

Shingo Bessho<sup>a</sup>, Kaitlyn C. M. Grando<sup>a</sup>, Kathrine Kyrylchuk<sup>a</sup>, Amanda Miller<sup>a</sup>, Andres J. Klein-Szanto<sup>b</sup>, Wenhan Zhu<sup>c</sup>, Stefania Gallucci<sup>d</sup>, Vincent Tam<sup>a</sup>, and Çağla Tükel<sup>a</sup>

<sup>a</sup>Center for Microbiology and Immunology, Lewis Katz School of Medicine, Temple University, Philadelphia, USA; <sup>b</sup>Histopathology Facility, Fox Chase Cancer Center, Philadelphia, PA, USA; <sup>c</sup>Department of Pathology Microbiology, and Immunology, Vanderbilt University Medical Center, Nashville, TN, USA; <sup>d</sup>Division of Innate Immunity, Department of Medicine, University of Massachusetts Chan Medical School, Worcester, MA, USA

## ABSTRACT

The *Salmonella* biofilm-associated amyloid protein, curli, is a dominant instigator of systemic inflammation and autoimmune responses following *Salmonella* infection. Systemic curli injections or infection of mice with *Salmonella* Typhimurium induce the major features of reactive arthritis, an autoimmune disorder associated with *Salmonella* infection in humans. In this study, we investigated the link between inflammation and microbiota in exacerbating autoimmunity. We studied C57BL/6 mice from two sources, Taconic Farms and Jackson Labs. Mice from Taconic Farms have been reported to have higher basal levels of the inflammatory cytokine IL – 17 than do mice from Jackson Labs due to the differences in their microbiota. When we systemically injected mice with purified curli, we observed a significant increase in diversity in the microbiota of Jackson Labs mice but not in that of the Taconic mice. In Jackson Labs, mice, the most striking effect was the expansion of *Prevotellaceae*. Furthermore, there were increases in the relative abundance of the family *Akkermansiaceae* and decreases in families *Clostridiaceae* and *Muribaculaceae* in Jackson Labs mice. Curli treatment led to significantly aggravated immune responses in the Taconic mice compared to Jackson Labs counterparts. Expression and production of IL – 1 $\beta$ , a cytokine known to promote IL – 17 production, as well as expression of *Tnfa* increased in the gut mucosa of Taconic mice in the first 24 hours after curli injections, which correlated with significant increases in the number of neutrophils and macrophages in the mesenteric lymph nodes. A significant increase in the expression of *Ccl3* in colon and cecum of Taconic mice injected with curli was detected. Taconic mice injected with curli also had elevated levels of inflammation in their knees. Overall, our data suggest that autoimmune responses to bacterial ligands, such as curli, are amplified in individuals with a microbiome that promote inflammation.

## ARTICLE HISTORY

Received 25 January 2023  
Revised 30 May 2023  
Accepted 31 May 2023

## KEYWORDS



*Salmonella*; curli; amyloid; biofilm; autoimmunity; microbiome; reactive arthritis

## Introduction


Amyloid proteins adopt a conserved cross beta-sheet structure and form fibrils through a self-assembly process.<sup>1</sup> More than 60 amyloidogenic proteins are expressed in humans, and the fibrillar deposits of some of these proteins are observed in patients with neurological and inflammatory diseases such as Alzheimer's disease, Huntington's disease, Parkinson's disease, type II diabetes, and secondary amyloidosis.<sup>2–4</sup> Amyloid proteins are also produced by bacteria and are detected within the extracellular matrix of their biofilms<sup>5</sup>. Curli, the best-studied bacterial amyloid, is produced by

enteric bacteria including *Escherichia coli* and *Salmonella enterica* serovar Typhimurium<sup>6,7</sup>. Curli tends to deposit in the extracellular matrix of biofilms formed by these bacteria. Bacterial amyloids provide a protective environment for bacteria in the biofilm community. Consistent with this idea, curli provides protection against bacteriophages, antibacterial agents, desiccation, and immune attacks.<sup>8–11</sup>

Although curli mainly acts as a barrier against environmental insults, it also plays a critical role in stimulating the host immune system. Curli is one of the first bacterial components the immune system

**CONTACT** Çağla Tükel  [ctukel@temple.edu](mailto:ctukel@temple.edu)  Center for Microbiology and Immunology, Lewis Katz School of Medicine, Temple University, 3500N. Broad St, Philadelphia, PA19140

VT and CT contributed equally to this work.

 Supplemental data for this article can be accessed online at <https://doi.org/10.1080/19490976.2023.2221813>

© 2023 The Author(s). Published with license by Taylor & Francis Group, LLC.

This is an Open Access article distributed under the terms of the Creative Commons Attribution-NonCommercial License (<http://creativecommons.org/licenses/by-nc/4.0/>), which permits unrestricted non-commercial use, distribution, and reproduction in any medium, provided the original work is properly cited. The terms on which this article has been published allow the posting of the Accepted Manuscript in a repository by the author(s) or with their consent.

encounters when dealing with a biofilm.<sup>9</sup> Curli accounts for about 85% of the extracellular matrix of enteric biofilms<sup>12</sup> and serves as a major pathogen-associated molecular pattern (PAMP) by triggering Toll-like receptor 2 (TLR2).<sup>13</sup> In contrast, in the invasive motile form, enteric bacteria strongly activate other immune receptors, including TLR4/MD2/CD14,<sup>14</sup> TLR5,<sup>15</sup> and a NOD-like receptor, NLRC4,<sup>16,17</sup> and lipopolysaccharide (LPS) and flagellin serve as the major PAMPs. Biofilm-associated bacteria do not express flagellin,<sup>18</sup> and although it is plausible that the curli deposits mask lipid A of LPS, which activates TLR4, it is not known whether immune cells can access these cell components to induce the inflammatory responses when bacteria are within a biofilm.

Fully formed, mature curli fibrils activate the heterocomplex of TLR2 and TLR1.<sup>13,19,19–21</sup> Furthermore, during biofilm establishment, curli binds to cellulose and extracellular DNA to increase the stability of the extracellular matrix.<sup>22</sup> Complexes formed between curli and DNA stimulate a stronger activation of immune cells than curli or DNA alone.<sup>23</sup> Purified curli/DNA complexes induce the upregulation of classical inflammatory cytokines such as IL – 6, IL – 12, IL – 17, and TNF $\alpha$  and induce the activation of type I interferon signaling and the subsequent expression of interferon-stimulated genes via TLR2 and TLR9 activation.<sup>13,19,23,24</sup> Curli/DNA complex activates the innate immune system in a two-step process: curli activates the TLR2/TLR1 heterocomplex,<sup>13,19,21</sup> and internalization of this complex brings the curli/DNA complex into the endosome where the DNA receptor, TLR9, is activated.<sup>22</sup> Curli and other fibrillar amyloids can escape the endosome and gain access to the cytosol, activating cytosolic immune receptors including the NLRP3 inflammasome leading to IL – 1 $\beta$  production.<sup>20</sup>

Recent work has suggested that expression of the bacterial amyloid curli in the gut by enteric bacteria might be linked to neurodegenerative and autoimmune diseases.<sup>25–28</sup> Although the mechanisms by which curli contributes to autoimmunity is not well understood, our previous studies suggest that the translocation of curli/DNA complexes from the gut to systemic circulation induces the production of pro-inflammatory markers, like TNF $\alpha$  and IL – 17, and the generation of anti-nuclearlike anti-double-

stranded DNA (anti-dsDNA), hallmarks of classical autoimmune responses.<sup>22,23,29</sup> Furthermore, gastrointestinal infections with curli-expressing enteric pathogens, including *S. Typhimurium*, *Campylobacter jejuni*, and *Yersinia enterocolitica*, are linked to the onset of reactive arthritis,<sup>29,30</sup> a human autoimmune disease that affects joints. Recent work established that in mice infected with *S. Typhimurium*, translocation of curli/DNA complexes from the gut is required for the generation of autoimmunity and joint inflammation.<sup>30</sup> Intriguingly, curli-expressing bacteria also participate in the pathogenesis of disease flares in patients with systemic lupus erythematosus (SLE). Persistent bacteriuria with uropathogenic *E. coli* and production of higher levels of anti-curli/DNA antibodies were detected in SLE patients with higher levels of markers of inflammation and increased disease severity,<sup>31</sup> suggesting that systemic exposure to bacterial curli/DNA complexes stimulates autoimmunity in patients with existing autoimmune conditions.

It has been reported that the systemic presence of PAMPs such as LPS or flagellin can affect the mucosal immune response leading to changes in the gut microbiome composition.<sup>32,33</sup> Here, we evaluated how systemic curli or enteric biofilm exposure alters the gut microbiome and the mucosal immune system in mice and the consequences of these changes on reactive arthritis. Since it has been reported that IL – 17 production and type 17 immunity are linked to autoimmunity,<sup>34</sup> and especially in the context of arthritis, we chose to test the effect of curli in C57BL/6 mice from Taconic Farms and from Jackson Labs, which have different basal levels of IL – 17 due to differences in their microbiota.<sup>35</sup> We investigated how curli exposure alters the gut microbiota and whether the presence of an IL – 17-promoting commensal influences the innate immune response against curli and the induction of autoimmunity.

## Results

### Systemic curli exposure alters the gut microbiota

We investigated the effect of systemic curli exposure on the gut microbiota of C57BL/6 mice from

Taconic Farms and from Jackson Labs. Due to microbiome differences, mainly the presence of Segmented Filamentous Bacteria (SFB), the mice from Taconic Farms have higher basal levels of the inflammatory cytokine IL-17 than do Jackson Labs mice.<sup>35</sup> Mice were housed in a BSL2 room. Cages from Jackson Labs and Taconic Farms were kept on different sides of the room and a designated person changed the cages on separate days to limit cross contamination. Microbiota was analyzed at week 0 and week 8 following housing only. Although a slight change in microbiota was detected by PCoA, no microbiota transmission between the two groups of mice was detected. We attribute these changes to the age of the mice or the facility effect (Supplementary Figure S1). Curli was purified as previously described with slight modifications,<sup>36</sup> resulting in a preparation that contains high levels of DNA and it is not cytotoxic.<sup>23,36,37</sup> The mice were injected intraperitoneally (i.p.) with 100 µg of curli or sterile PBS twice a week for eight weeks. To characterize the gut microbiota, 16S rRNA profiling was performed on DNA extracted from the cecal contents of mice at week 8. The V3-V4 region of 16S rRNA was sequenced using Illumina MiSeq system. There were no significant differences in the microbiome composition of Taconic mice injected with sterile PBS nor curli; however, Jackson Labs mice injected with curli had a significantly altered microbiota compared to control mice injected with sterile PBS (Figure 1a). Principal coordinate analysis (PCoA) on the family level of microbiota composition showed clustering of the Taconic mice regardless of treatment, whereas, for the Jackson Labs mice, the PCoA showed a distinct clustering of samples from control versus curli-treated mice (Figure 1b).

No significant differences were detected in the Firmicutes/Bacteroidetes ratio, an indication of gut dysbiosis, in samples from different groups (Figure 1c). To investigate the differences in alpha diversity, Shannon entropy and Faith's phylogenetic diversity were calculated. Although no significant differences were observed based on Shannon entropy (Figure 1d), Faith's phylogenetic diversity, an alpha diversity index based on phylogenetic distances, showed a significant increase in microbiome diversity

in curli-treated Jackson Labs mice compared to the control (Figure 1e). Furthermore, control Taconic mice had higher phylogenetic alpha diversity compared to control Jackson Labs mice; this was also the case for curli-treated group (Figure 1e).

Notably, *Tannerellaceae*, *Prevotellaceae*, and *Rickenellaceae* were not detected in the cecal samples of control Jackson Labs mice; however, these taxa were present in high abundance in both groups of the Taconic mice (Figure 1a,f,g). Moreover, these taxa were significantly expanded in Jackson Labs mice treated with curli compared to PBS-treated controls (Figure 1a,f,g). *Bacteroidaceae* species were present at higher abundance in samples from control Jackson Labs mice compared to curli-treated Jackson Labs mice and to both Taconic groups (Figure 1a,f,g). Lastly, upon curli treatment, the abundance of *Erysipelotrichaceae* was increased only in the Jackson Labs mice (Figure 1a,f,g). The abundance of *Erysipelotrichaceae* was lower in control Taconic mice than in control Jackson Labs mice (Figure 1g). Overall, upon treatment with curli, the composition of the cecal microbiota in Jackson Labs mice changed toward resembling the Taconic microbiota.

### **The variation and the multitude of curli-induced microbiota changes depend on the resident microbiota**

In addition to cecal contents, we also analyzed the microbiota composition of fecal samples before and after curli injections using 16S rRNA profiling. *Erysipelotrichaceae* were more abundant in the fecal microbiota of Jackson Labs mice compared to Taconic mice (Figure 2a,b,i,j). *Lachnospiraceae* and *Lactobacillaceae* abundance was higher in the fecal microbiota of Taconic mice compared to Jackson Labs mice prior to curli treatment and was increased in the feces of Jackson Labs mice upon injection with curli (Figure 2a,b,i,j). *Prevotellaceae* and *Ricknellaceae* abundances were low in the fecal samples of control and curli-treated Jackson Labs mice (Figure 2a,i). These taxa were present in the Taconic mice microbiota regardless of curli treatment (Figure 2b,i). As observed in the cecal microbiota, curli treatment resulted in very little change in the composition of the fecal microbiota of Taconic mice; only

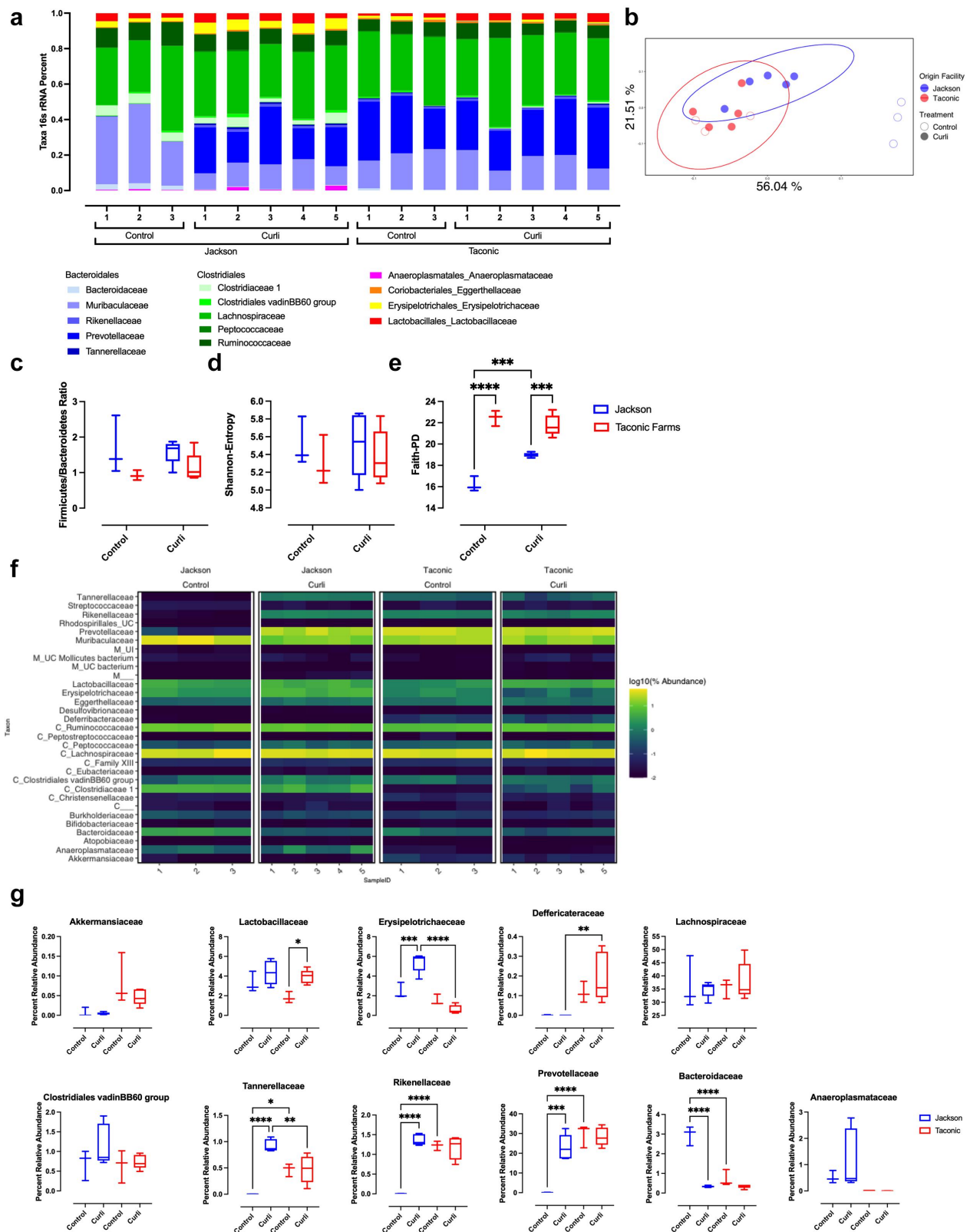


**Figure 1.** The effect of systemic curli treatment on composition of cecal bacterial community. (a) Bacterial taxa present in DNA extracted from cecal contents of C57BL/6 mice from Jackson Labs and Taconic treated with curli or PBS for eight weeks as determined by 16S profiling. (b) PCoA of microbiota composition (weighted UniFrac distances). (c) Firmicutes and Bacteroidetes ratio. Alpha diversity of microbiota composition represented by (d) Shannon entropy and (e) Faith's phylogenetic diversity. Significance was analyzed by two-way ANOVA and multiple comparison; \*\*\* $p < 0.001$ , \*\*\*\* $p < 0.0001$ . (f) Heatmap of the top 30 most abundant taxa. (g) Abundances of indicated species. Significance was analyzed using one-way ANOVA and multiple comparison; \* $p < 0.05$ , \*\* $p < 0.01$ , \*\*\* $p < 0.001$ , \*\*\*\* $p < 0.0001$ .



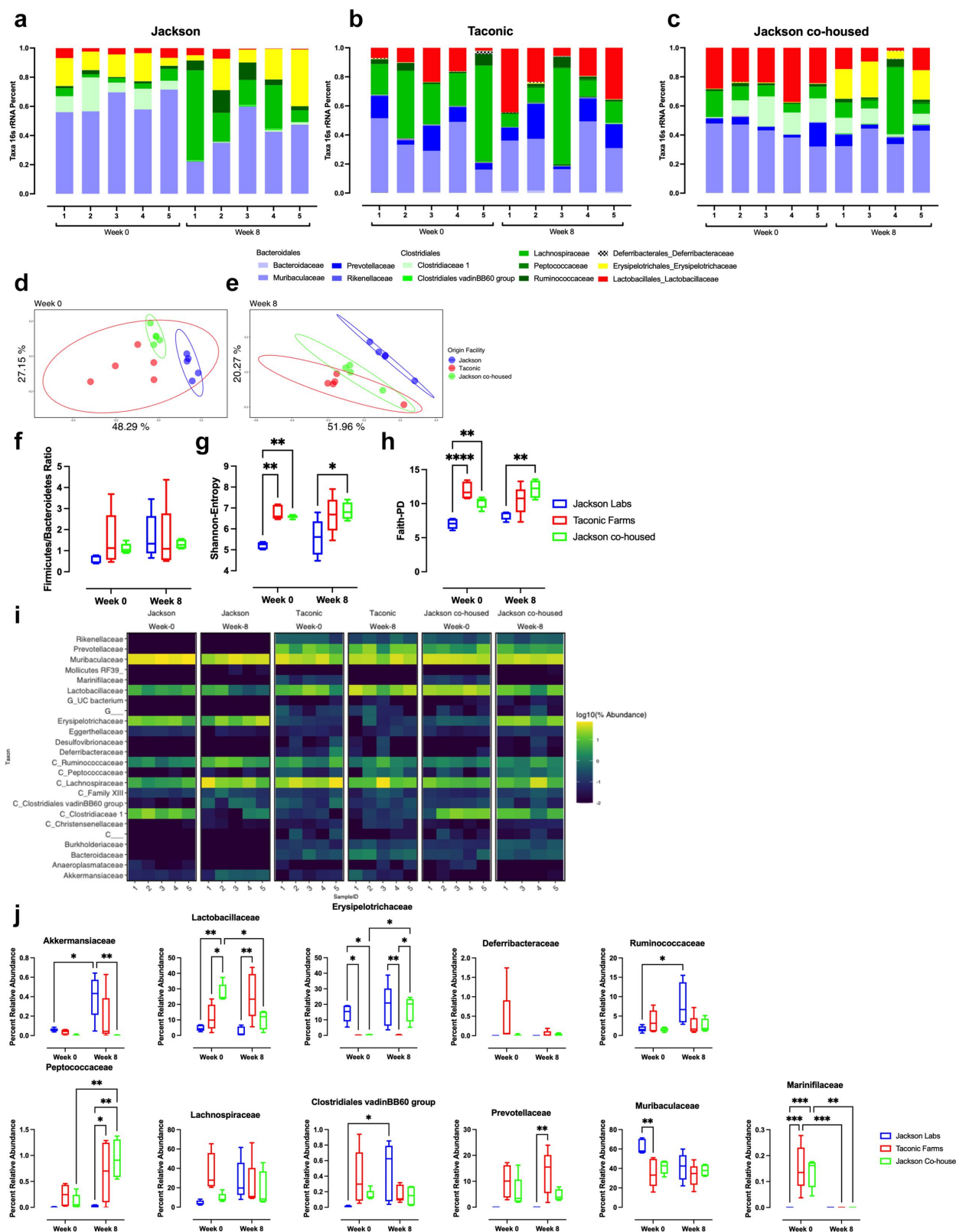


**Figure 2.** The effect of systemic curli treatment on the composition of the bacterial community in feces. Bacterial taxa present in DNA extracted from feces of C57BL/6 mice from (a) Jackson Labs, (b) Taconic or (c) mice from Jackson labs that were co-housed with Taconic mice for 3 weeks. Mice were treated with curli for eight weeks as determined by 16S profiling. Level 5 microbiota composition. (d) PCoA of microbiota composition at week 0 before treatment or (e) at week 8 (weighted UniFrac distances). (f) Firmicutes and Bacteroidetes ratio. Alpha diversity of microbiota composition represented by (g) Shannon entropy and (h) Faith- phylogenetic diversity. (i) Heatmap of the top 30 most abundant taxa. (j) Abundances of indicated species. Alpha diversity was analyzed using 2-way ANOVA and multiple comparison  $p < 0.05$ ,  $**p < 0.01$ ,  $***p < 0.0001$ . Abundance was analyzed using One-way ANOVA and multiple comparison  $p < 0.05$ ,  $**p < 0.01$ ,  $***p < 0.001$ .

a significant decrease in *Marinifilaceae* was observed (Figure 2b,i,j).

Next, we co-housed Jackson Labs mice with Taconic mice for three weeks prior to i.p. injection with purified curli/DNA twice a week for eight weeks. We confirmed the transfer of SFB from Taconic mice to Jackson mice via qPCR using the fecal DNA (Supplementary Figure S1). PCoA of the microbiota composition showed the clustering of untreated co-housed Jackson Labs mice with untreated Taconic mice rather than with untreated non-co-housed Jackson Labs mice (Figure 2d). These data indicated the success of gut microbiota transfer (Figure 2a–c). In addition, curli-treated co-housed Jackson Labs mice had a microbiota that clustered with curli-treated Taconic mice (Figure 2e).

Although not statistically significant, a lower Firmicutes/Bacteroidetes ratio in the fecal microbiota of untreated Jackson Labs mice was detected when compared to all other groups (Figure 2f). There were significant differences in alpha diversity based on Shannon entropy and Faith's phylogenetic diversity score between untreated Jackson Labs mice, Taconic mice, and co-housed Jackson Lab mice; however, there was not a significant difference between curli-treated co-housed Jackson Labs mice and curli-treated Taconic mice (Figure 2g,h). This increase in alpha diversity of co-housed Jackson Labs mice upon curli treatment suggests that curli increased the richness of the gut ecosystem of Jackson Labs mice, while it did not significantly change the microbiota of the Taconic mice.

In the fecal microbiota, *Lactobacillaceae*, *Lachnospiraceae*, *Clostridiales* vadinB660, *Marinifilaceae*, *Prevotellaceae*, and *Peptococcaceae* were detected at lower abundances in untreated Jackson Labs mice compared to other groups. After curli injections, there were significant increases in the relative abundances of *Akkermansiaceae*, *Ruminococcaceae*, and *Clostridiales* vadinB660 group in Jackson Labs mice (Figure 2i,j). Simultaneously, there was a loss of significant difference in the relative abundance of *Muribaculaceae* between Jackson Labs and Taconic mice after curli injections (Figure 2i,j). Untreated co-housed Jackson Labs mice had a microbiome profile similar

to that of untreated Taconic mice, however, statistically significant changes were only seen in co-housed Jackson Labs mice. Curli-treated co-housed Jackson Labs mice had significant increases in *Erysipelotrichaceae* and *Peptococcaceae* and significant decreases in *Lactobacillaceae* and *Marinifilaceae* when compared to the untreated co-housed Jackson Labs mice (Figure 2i,j). These data indicate that curli triggers changes in the gut microbiota that are affected by the resident microbiota.

### Systemic curli exposure changes the gut immune responses

The activation of the TLR2/TLR1 receptor complex by curli strongly induces the expression of several cytokines including IL – 6, IL – 12, IL – 17, and TNF $\alpha$ .<sup>13,19,23,24,37</sup> Upon TLR2 activation, curli is taken up by immune cells and escapes to the cytosol where it activates the NLRP3 inflammasome leading to the production of IL1 $\beta$ .<sup>20</sup> Additionally, curli and the DNA associated with this amyloid together induce the activation of the type I interferon signaling and the expression of interferon-stimulated genes as well as a strong anti-dsDNA autoantibody response.<sup>22,23,37</sup>

To determine whether the changes we observed in the microbiota of the Jackson Lab mice upon curli treatment could be due to changes in the mucosal immune responses, we investigated the gene expression patterns in the cecum, colon, and mesenteric lymph nodes of C57BL/6 mice from Jackson Labs and Taconic Farms injected i.p. with 100  $\mu$ g of curli/DNA or sterile PBS. Organs were collected 24 hours after injection, RNA was isolated, and qPCR was performed. *Il – 1b* expression was significantly increased in the cecum, colon, and mesenteric lymph nodes of Taconic mice injected with curli compared to mice that were injected with PBS (Figure 3a–c). Increased *Tnfa* expression was also observed in the colon and mesenteric lymph nodes of Taconic mice injected with curli compared to mice injected with PBS, but no significant differences in *Il – 10* or *Il – 6* expression were observed in the gut tissues (Figure 3a–c). Although there was an increase in *Il – 1b* and *Tnfa* in the colon and cecum of Jackson Labs mice treated with curli,

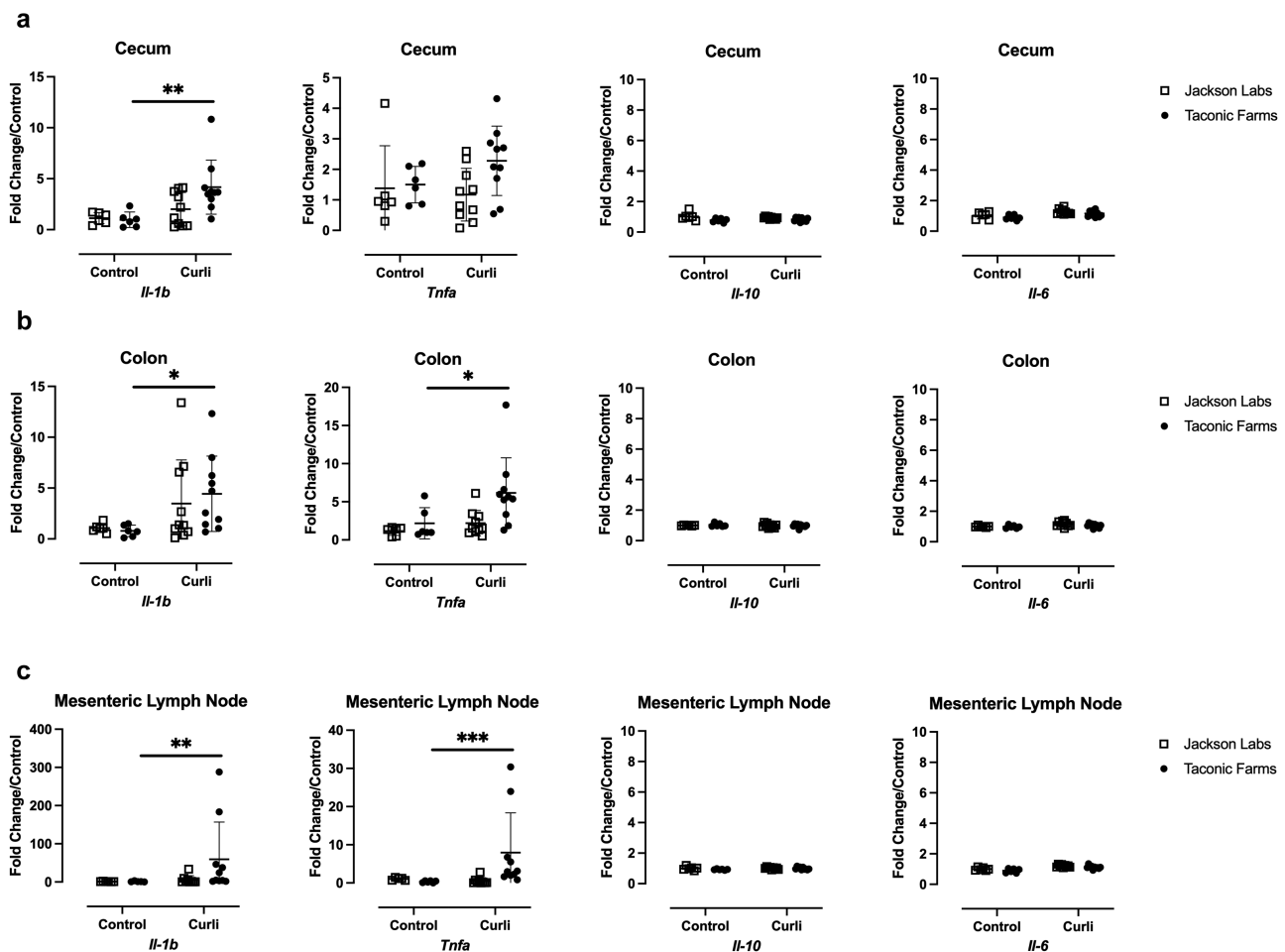


**Figure 3.** The effect of curli on levels of cytokine mRNAs in cecum, colon, and mesenteric lymph node. Levels of *Il-1b*, *Tnfa*, *Il-10*, and *Il-6* determined by RT-qPCR in RNA extracted 24 hours after indicated treatment from (a) cecum (b) colon, and (c) mesenteric lymph node of C57BL/6 mice from either Jackson Labs or Taconic Farms. Data were normalized to data from Jackson Labs mice treated with PBS. Each data point represents one mouse sample. Mean and standard error were calculated by averaging results from two independent experiments. Significance was determined using a Mann-Whitney test; \* $p < 0.05$ , \*\* $p < 0.01$ , \*\*\* $p < 0.001$ .

the expression levels of these cytokines were not significantly different from mice injected with PBS (Figure 3a–c). In the spleen, the expression of *Il-1b* was also significantly increased in curli-injected Taconic mice compared to PBS-treated Taconic mice and to curli-treated Jackson Labs mice (Figure 4a). At this time point, no differences in *Il-6* expression were detected in the spleen (Figure 4a).

To confirm that the increased *Il-1b* expression translated into mature IL-1 $\beta$  production in the gut mucosa, mature IL-1 $\beta$  protein levels were measured in the cecum and colon tissue homogenates by ELISA. A significant increase in the production of IL-1 $\beta$  in the cecum of both Jackson Labs and Taconic mice was confirmed (Figure 4b). In the colon, a significant

increase in IL-1 $\beta$  was only detected in Taconic mice upon curli treatment (Figure 4b) confirming the expression results observed in Figure 3. These results indicate that the systemic exposure to curli affects the expression of immune cytokines at the mucosal sites, where they may influence and be influenced by the microbiota composition.

Fecal IgA levels were also evaluated. Although the IgA levels were higher in Taconic mice compared to Jackson Labs animals in the absence of treatment, no significant differences were induced upon curli treatment for two or eight weeks (Figure 4c). These changes in cytokine expression in the gut mucosa upon exposure to curli suggest that the immune activation following systemic curli exposure modulates changes in gut microbiota.

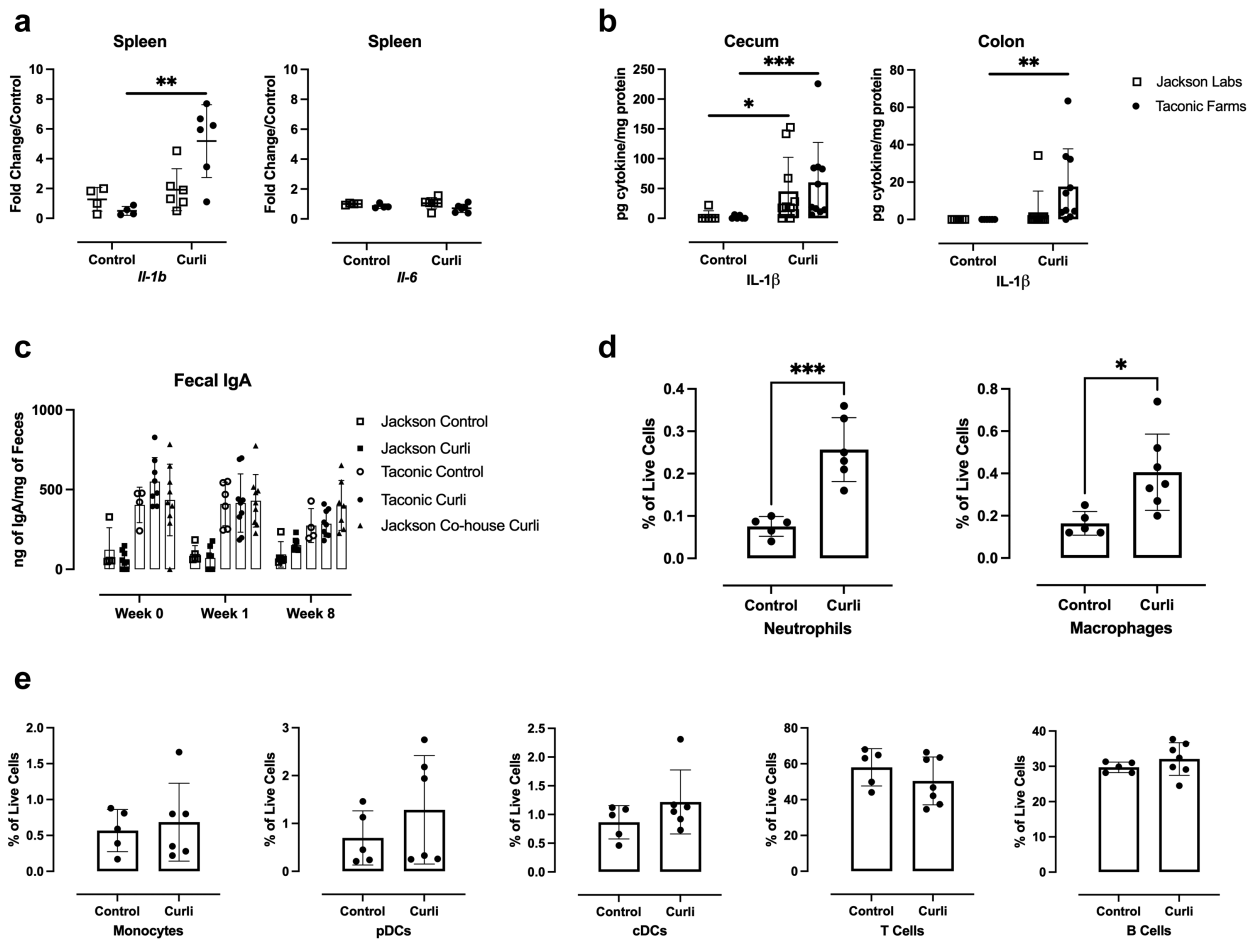


**Figure 4.** Immune responses in the spleen, gut, and mesenteric lymph nodes in response to curli treatment. (a) Levels of IL-1 $\beta$  and IL-6 determined by RT-qPCR in spleens of mice sacrificed 24 hours after injection with 100  $\mu$ g curli or PBS (control). Data were normalized to data from control mice from Jackson Labs. (b) Concentration of IL-1 $\beta$  protein from cecum and colon as determined by ELISA in mice treated as in panel a. (c) Concentration of IgA determined by ELISA in fecal pellets collected at indicated times of treatment with curli. Flow cytometry analysis of mesenteric lymph node cell suspensions for (d) T and B cells were gated using CD3 and CD19, respectively and (e) innate immune cells were gated using CD11b, F4/80, Ly6G, B220, CD11c, and Ly6C. Cells were gated after elimination of doublets and dead cells. Means and standard errors were calculated by averaging results from two independent experiments. Statistical significance was determined using a Mann-Whitney test; \* $p < 0.05$ , \*\* $p < 0.01$ , \*\*\* $p < 0.001$ .

### Immune cell populations

To identify the immune cell populations that shape the observed mucosal responses, we investigated the cell populations in mesenteric lymph nodes of Taconic mice using flow cytometry. No changes were detected in the number of T and B cells, plasmacytoid dendritic cells, conventional dendritic cells, migratory dendritic cells, or monocytes at 24 hours after curli injection (Figure 4d,e). However, we did detect a significant increase in neutrophils and macrophages in Taconic mice treated with curli when compared to PBS-treated animals (Figure 4e), compatible with the first wave of inflammatory phagocytes called to the site of infection and then migrating to the

draining lymph nodes. To determine the chemokines involved in the chemoattraction of these innate cells, we measured the gene expression of chemokines required to recruit neutrophils, and found a significant increase in the expression of *Ccl3* in colon and cecum of Taconic mice injected with curli (Figure 5a,b). While there was also an increase in the *Cxcl5* and *Cxcl1* expression in the cecum of Taconic mice injected with curli compared to control animals, these differences did not reach significance (Figure 5a,b). The expression of *Cxcl5* in the colon was also elevated both in Jackson mice and Taconic mice upon curli injection, but these differences did not reach significance (Figure 5a,b).



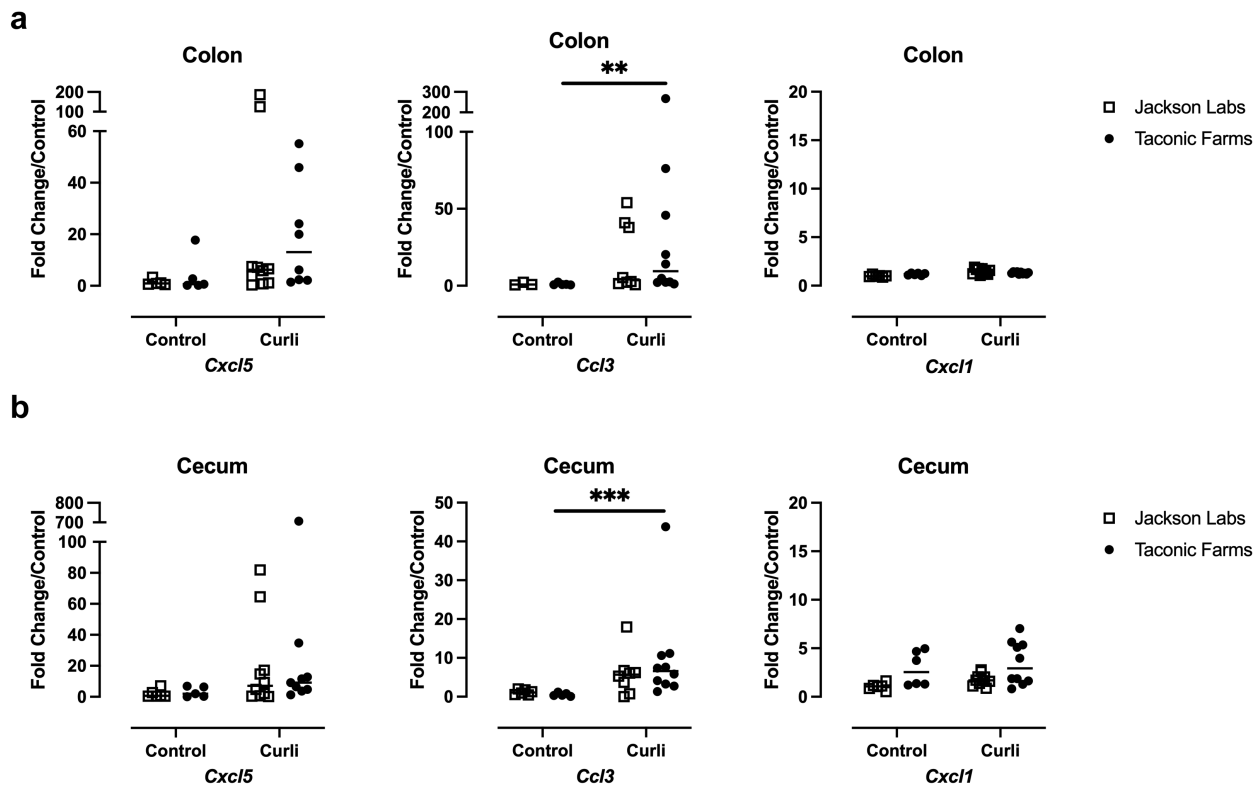


**Figure 5.** Expression of chemokines in the cecum and colon. Levels of Cxcl5, Ccl3, and Cxcl1 determined by RT-qPCR in RNA extracted 24 hours after indicated treatment from (a) colon and (b) cecum of C57BL/6 mice from either Jackson Labs or Taconic Farms. Data were normalized to data from Jackson Labs mice treated with PBS. Each data point represents one mouse sample. Mean and standard error were calculated by averaging results from two independent experiments. Significance was determined using a Mann-Whitney test; \*\* $p < 0.01$ , \*\*\* $p < 0.001$ .

We have previously shown that purified curli/DNA complexes induce a strong autoantibody response against DNA, even in C57BL/6 mice;<sup>22,23,37</sup> therefore, we evaluated levels of the anti-dsDNA autoantibodies induced by curli in Jackson Labs and Taconic mice. Regardless of their facility of origin, there was a significant increase in anti-dsDNA IgG production in mice after two weeks of treatment with curli compared to mice injected with PBS, and there were no significant differences in the levels of anti-dsDNA IgG autoantibodies between Jackson Labs mice and Taconic mice (Figure 6a). At this time point of 8 weeks, while CD4<sup>+</sup> and CD8<sup>+</sup> T cell populations had no significant difference between control and curli treated mice regardless of facility origin, there was a significant increase in ICOS<sup>+</sup> T cells in the spleen of Taconic mice treated with curli compared to the control mice and Jackson Labs mice (Figure 6b). There were no changes in the percentage of overall B cells, plasmablasts and plasma

cells, however, there was a significant increase in germinal center B cell population in the spleen of Taconic mice treated with curli when compared to the control mice and Jackson Labs mice (Figure 6c), suggesting that the similar induction of autoantibodies in the two groups of mice may rely on different mechanisms, and only Taconic mice develop detectable numbers of GC B cells upon curli exposure.

Next, we examined the induction of arthritis by curli, as we have previously reported.<sup>30</sup> The knee inflammation was scored for synovial hyperplasia, chronic inflammation, periosteal resorption, and dilated articular cavity in the curli- and PBS-injected mice after three weeks of treatment with curli or PBS by a pathologist in a blinded study. Intriguingly, Taconic mice injected with curli exhibited significantly increased pathology compared to mice injected with PBS (Figure 6d). It is important to note

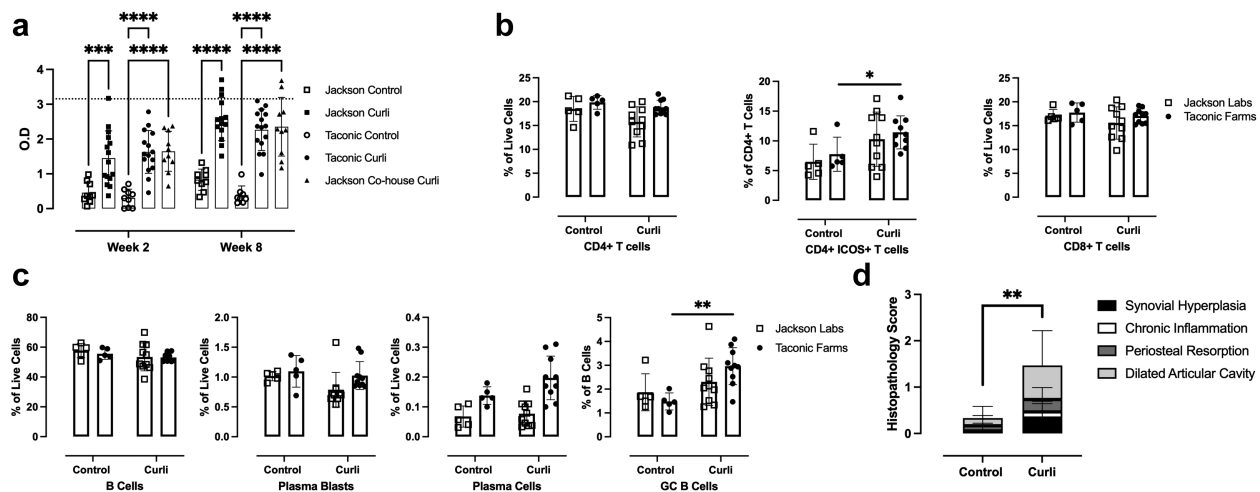


**Figure 6.** Effects of curli on the generation of anti-dsDNA autoantibodies and joint inflammation. (a) Mean levels of anti-dsDNA autoantibodies in mouse serum, quantified by ELISA, from mice treated with curli or PBS for 8 weeks. Flow cytometry analysis of splenocytes for (b) T cells were gated using CD3, CD4, and inducible T cell co-stimulator (ICOS) and (c) B cells were gated using CD45R, CD138, and CD95. (d) Blinded histopathology score from knee joints of Taconic mice treated with curli or PBS for 8 weeks. The following scale was used: 0, no change; 1, slight changes; 2, moderate changes; 3, severe changes. Mean and standard error were calculated by averaging results from two independent experiments.  $^{**}p < 0.01$  as determined by one-way ANOVA.

that C57BL/6 mice are resistant to joint inflammation and arthritis.<sup>30,38</sup> No differences were noted for Jackson mice (data not shown).

## Discussion

Complex biological communities of bacteria, known as biofilms, dominate all habitats including the human gastrointestinal tract.<sup>39</sup> Bacteria embedded in biofilms thrive in the intestinal tract enduring environmental and immune pressures while competing with other members of the microbiota. Studies have shown that upon the transition into a biofilm, bacteria go through a metabolic reprogramming that changes the physiology and biology of the individual bacterial cells.<sup>40</sup> The biofilm extracellular matrix contains unique components that protects the bacterial community by providing a strong and impenetrable shield.<sup>41</sup> Medical microbiologists became interested in the biofilm lifestyle of organisms when a link between the etiology of a persistent infection and aggregates of bacteria were established in cystic fibrosis patients in the early 1970s.<sup>42</sup> Since then, biofilms have been recognized to be involved in many clinical infections,<sup>43</sup> and evidence is accumulating that biofilms contribute to the pathogenesis of not only chronic infections but also acute bacterial infections.<sup>44–46</sup>

Amyloid/DNA complexes are detected in biofilms of numerous bacteria, both commensal and pathogenic. Though the amyloid proteins themselves differ in primary amino acid sequence, all self-assemble into a conserved beta-sheet structure and associate with DNA.<sup>23,29,47–49</sup> Recent work suggests that chronic systemic exposure to biofilms or to the amyloid/DNA complexes from Gram-negative or Gram-positive bacteria, curli/DNA and PSM/DNA, respectively, are associated with the generation of autoimmune responses both in mice and humans.<sup>22,23,25,31,37,49,50</sup> Curli is produced in the gastrointestinal tract by Gram-negative enteric bacteria<sup>37</sup> and serves as a major biofilm-associated PAMP.<sup>9,13,19,21,24,51</sup> During invasive *S. Typhimurium* infection, curli/DNA complexes leak through the damaged epithelial barrier to trigger the generation of anti-dsDNA autoantibodies and joint inflammation in mouse models of infection.<sup>23,37</sup> Thus, curli may underlie the pathogenesis of reactive arthritis, an autoimmune disease that occurs in 5% of the patients following acute *Salmonella*-induced gastroenteritis.<sup>8,23,29,37</sup> In addition to *Salmonella*, curli/DNA complexes from commensal *E. coli* also cause lupus-like autoimmune manifestations and inflammation once they are introduced systemically bypassing the gut.<sup>23</sup> Consistent with these findings, recent studies suggest that bacterial

PAMPs from the chronic infections, coupled with genetic susceptibility can fuel abnormally strong inflammatory reactions to bacterial curli.<sup>31</sup>

Since many evidence support that the IL – 17-mediated response is linked to autoimmunity,<sup>34,52–54</sup> we tested the effect of curli in C57BL/6 mice from Taconic Farms and from Jackson Labs as mice from these vendors have different basal levels of IL – 17 due to differences in their microbiota.<sup>35</sup> Taconic mice, which have higher basal levels of IL – 17 due to the presence of segmented filamentous bacteria than do mice from Jackson Labs,<sup>35</sup> were more resistant to curli-induced changes in the gut microbiome. Similar to two other bacterial PAMPs, LPS and flagellin,<sup>32,33,54</sup> systemic curli exposure led to significant changes in the microbiota composition of mice from Jackson Labs. Treatment with curli in Jackson Labs mice increased the abundance of *Erysipelotrichaceae*, *Tannerellaceae*, *Rikenellaceae*, and *Prevotellaceae* and decreased the abundance of *Bacteroidaceae* in the cecal contents of these mice. Intriguingly, *Prevotellaceae* was previously linked to rheumatoid arthritis and Th17 responses in humans.<sup>55</sup> Curli was previously linked to IL – 17 production in Jackson Labs mice,<sup>24</sup> but further studies will be needed to determine whether the presence of curli in the gut leads to higher IL – 17 responses directly or indirectly due its effects on other microbial populations.

Co-housing of the Jackson Labs mice with mice from Taconic for 3 weeks resulted in alterations of the microbiota of the Jackson Labs mice to a profile similar to that of the Taconic mice. It remains to be elucidated why the microbiota from Taconic mice is dominant. The curli-treated, co-housed Jackson Labs mice had microbiomes more similar to the untreated control and curli-treated Taconic mice groups than to the non-co-housed, curli-treated Jackson Labs mice, indicating that the transfer of the Taconic microbiota resulted in a microbiota more resistant to changes upon curli treatment. Curli treatment of the co-housed Jackson Lab mice resulted in the expansion of two families, *Erysipelotrichaceae* and *Peptococcaceae*. Previous studies showed that *Ruminococcus gnavus*, a member of *Peptococcaceae*, was of higher abundance in lupus nephritis patients than in healthy

subjects,<sup>56</sup> suggesting that the *Peptococcaceae* may be associated with inflammatory processes and autoimmunity.

Next, we sought to determine whether the changes to the microbiota composition were associated with higher gut mucosal immune response in Jackson Labs mice. To our surprise, after curli treatment, higher cytokine expression was detected in cecum, colon, and mesenteric lymph nodes of Taconic mice compared to Jackson Labs mice. Although previous studies showed that curli increased pre-IL – 1 $\beta$  and mature IL – 1 $\beta$  in cultured macrophages via TLR2 and NLRP3 inflammasome activation, respectively, our study is the first to report *in vivo* production of IL – 1 $\beta$  in the intestinal mucosa upon curli stimulation. One dose of curli increased the production of IL – 1 $\beta$  in both groups of mice, but the levels were higher in Taconic mice than in mice from Jackson Labs. As inflammasome-derived IL – 1 $\beta$  induces IL – 17 responses,<sup>57</sup> it is not surprising that this cytokine was detected at higher levels in Taconic mice as these mice produce higher levels of IL – 17 upon stimulation by bacterial infection than do the mice from Jackson Labs, and therefore may be prone to producing more IL – 1 $\beta$  upon exposure to curli.<sup>35</sup> Our results suggest that a pro-inflammatory microbiota predisposes to strong immune responses to biofilms and participate to predispose to autoimmunity.

When we investigated the innate immune cells in the mesenteric lymph nodes of Taconic mice by flow cytometry, we discovered that the numbers of neutrophils and macrophages were increased 24 hours following a single curli injection. This result represents the first wave of inflammatory phagocytes called to the site of infection and also migrating to the draining lymph nodes. No changes were detected in the number of T and B cells, plasmacytoid dendritic cells, conventional dendritic cells, or monocytes, events that represents the second wave of immune cells, which is expected to occur in the following 3–7 days. It is important to note that IL – 1 $\beta$  production by neutrophils was recently demonstrated to drive epithelial shedding in a multi-component human intestinal organoid model of *Salmonella* infection.<sup>58</sup> Taken together, these results suggest that the curli produced by *Salmonella* while building their biofilms in the

intestinal tract may be a molecular signal that initiates epithelial shedding to control bacterial numbers during infection and prevent biofilm attachment to the epithelia, a potential powerful mechanism in the host defense against biofilms. Alternatively, this type of response could be specifically triggered by *Salmonella* to increase inflammation and transmission. Additional studies are needed to test these scenarios and determine if the presence of curli in the lumen induces IL-1 $\beta$  during oral infection. IL-1 $\beta$  and other IL-1-like cytokines have been implicated in the pathogenesis of autoimmune diseases including rheumatoid arthritis, psoriasis and SLE, and the induction of these cytokines by curli may suggest a novel pathogenetic step in these diseases.<sup>59,60</sup>

The analyses of immune cells after 8 weeks of chronic systemic exposure to curli revealed an unimpressive lack of alterations in the immune profile, with normal percentages of CD4+ and CD8+ T cells; B cell and plasma cell populations remained also stable, apparently unaltered by curli at this stage, suggesting that in non-autoimmune mice the induction of autoantibodies does not lead to detectable abnormalities in the general T and B cell subpopulations. Since we used C57BL/6 mice with a normal T and B cell repertoire, it should not be surprising that the presence of autoimmune lymphocytes cannot alter the total number of lymphocytes under the limitation of the techniques that we have used here. These results are mirrored by the similar levels of anti-dsDNA IgG autoantibodies that we measured in C57BL/6 mice from both Taconic and Jackson Labs Facilities upon curli treatment. These similarities suggest that the differences in microbiota and levels of the innate responses, found in mice from the two vendors, do not directly affect the autoantibody levels, which were induced by curli at similar levels than we found in previous reports.<sup>23,37</sup>

It is worthy to discuss the CD4+ICOS+ T follicular help cells (TFH) and GC B cells that were found to be significantly increased only in Taconic mice treated with curli. In canonical humoral immune responses, TFH provides help to B cells to become Antibodies-Forming Cells and isotype switch to produce IgG against specific antigens.<sup>61</sup> These activated B cells carry the characteristic markers of GC B cells. The results that

Taconic mice have significantly increased levels of both TFH and GC B cells upon curli treatment suggest that the induction of autoantibodies in Taconic mice follows the follicular activation of Ag-specific B cells. On the contrary, we found that curli treatment did not induce a significant increase in TFH and GC B cells in Jackson Labs mice compared to control Jackson mice. These results suggest that the induction of autoantibodies in Jackson mice does not follow the canonical activation of Ag-specific B cells, but it may occur extrafollicularly. The extrafollicular activation of autoreactive B cells has been previously suggested in murine lupus<sup>61,62</sup> and we had observed the extrafollicular activation of autoreactive B cells by curli in an independent project (Lee et al, *submitted manuscript*). Moreover, B cell responses to *Salmonella* had been shown to occur massively at extrafollicular sites, without notable germinal centers (GCs), as novel host defense mechanism.<sup>63,64</sup> These results prompt us to speculate that the production of autoreactive anti-dsDNA IgG induced by curli can occur via two different mechanisms, follicular and extrafollicular, depending on the state of immune activation, TH1 vs. TH17, and the quality of the microbiome. Future experiments will challenge this audacious hypothesis.

Although C57BL/6 mice are resistant to developing arthritis,<sup>38</sup> in the curli-treated Taconic C57BL/6 mice where higher IL-1 $\beta$  was detected in the gut, we observed increased joint inflammation. As IL-1 $\beta$  acts as a promoter for Th17-type immunity, which is linked to the development of autoimmunity, our results suggest an axis of IL-1 $\beta$ , IL-17 and autoimmune arthritis. We can speculate that in individuals with increased type-17 immunity, due to their microbiomes or genetic predisposition, curli- or biofilm-induced autoimmune reactions may be amplified. As it has been shown that IL-1 and IL-17 are therapeutic targets in Rheumatoid Arthritis and other inflammatory types of arthritis, our results suggest that these cytokines may have a pathogenic role in reactive arthritis after *Salmonella* infection, and provide a testable culprit, namely the exposure to bacterial amyloids like curli, for the up-regulation of IL-1 and IL-17 in reactive arthritis.

In conclusion, our data indicate that the microbiome strongly influences post-infectious autoimmunity and possibly the onset or flares of classical autoimmune diseases.

## Materials and methods

### Purification of curli

Curli aggregates were purified from the *S. Typhimurium* IR715  $\Delta msbB$  mutant<sup>65</sup> using a previously described protocol with slight modifications.<sup>36</sup> Briefly, an overnight culture of *S. Typhimurium* IR715  $\Delta msbB$  was grown in LB with appropriate antibiotic selection with shaking (200 rpm) at 37°C. Overnight cultures were then diluted in yeast extract supplemented with casamino acids (YESCA) broth with 4% DMSO to enhance curli production.<sup>36,65</sup> Bacterial cultures were grown in 150 ml of liquid YESCA medium containing 4% DMSO in a 250-ml flask. These cultures were grown at 26°C for 72 h with shaking (200 rpm). Bacterial pellets were collected by centrifugation, resuspended in 10 mM Tris-HCl (pH 8.0), and treated with 0.1 mg/ml RNase A from bovine pancreas (Sigma, R5502), 0.1 mg/ml DNase I (Sigma, DN25), and 1 mM MgCl<sub>2</sub> for 20 min at 37°C. Bacterial cells were then lysed by sonication (30% amplification for 30 s twice). Next, lysozyme was added (1 mg/ml; Sigma, L6876), and samples were incubated at 37°C. After 40 min, 1% SDS was added, and the samples were incubated for 20 min at 37°C with shaking (200 rpm). After this incubation, the curli-containing material was pelleted by centrifugation (10,000 rpm in a J2-HS Beckman centrifuge with rotor JA – 14 for 10 min at 4°C) and then resuspended in 10 ml Tris-HCl (pH 8.0) and boiled for 10 min. A second round of enzyme digestion with DNase, RNase was then performed as described above. The curli aggregates were then pelleted, washed with 10 mM Tris-HCl (pH 8.0), and resuspended in 2× SDS-PAGE buffer and boiled for 10 min. The samples were then electrophoresed on a 12% separating/3 to 5% stacking gel run for 5 h at 20 mA (or overnight at 100 V). Fibrillar aggregates are too large to pass into the gel and therefore remain within the well of the gel and can be collected. Once collected, the curli aggregates were washed three times with sterile

water and then extracted twice with 95% ethanol. Curli preparations were then resuspended in sterile water. Concentrations of curli aggregates were determined using the BCA assay according to the manufacturer's instructions (Novagen, 71285–3). Curli preparations were adjusted to have a protein concentration of 1 mg/ml.

### Treatment of mice

Female C57BL/6 (wild type) mice were purchased from Jackson Labs or Taconic Farms at 4–6 weeks old. At 6–8 weeks of age, mice were injected i.p. with 100 µg of curli/DNA complex or sterile PBS (control) twice a week, alternating sides for 8 weeks. For the 24-hour time point, mice were injected once and sacrificed 24 hours later. For the two-week time point, mice received four injections and were sacrificed 48 hours after the second injection.

### DNA extraction

Cecal contents and fecal pellets were collected and snap frozen in liquid nitrogen. Samples were stored at – 80°C until processing. DNA was extracted from samples using DNeasy PowerSoil Pro Kit (Qiagen) according to the recommendations of the manufacturer.

### 16S rRNA gene sequencing

Libraries were prepared from DNA isolated from cecal contents or fecal pellets and were sequenced at SeqMatic using an Illumina MiSeq system. The V3-V4 hypervariable region of 16S rRNA coding sequences was used to identify the bacteria. Data were subjected to a previously described workflow for processing.<sup>66,67</sup> The downstream analysis was performed with QIIME2 version 2022.2. Taxonomic profiling was performed against SILVA version 132.

### Detection of segmented filamentous

100 µg of bacterial DNA isolated from fecal pellets were used to run qPCR on Applied Biosciences StepOne Plus Real Time PCR system as described previously.<sup>68</sup> Primers used were: SFB736F – GACGCTGAGGCATGAGAGCAT, SFB844R – GACGGCACGGATTGTTATTCA, Eubact



**Table 1.** Antibodies used for FACS.

Marker, fluorophore, and clone number	Vendors and catalog numbers
<i>Fixable Viability Dye eFluor™ 780</i> , CD19 PE (1D3), CD3 APC (145-2C11), CD11b PE-Cy7 (M1/70), F4/80 Alexa Fluor® 488 (BM8), CD206 BV421 (C068C2), CD86 eFluor450 (GL1)	Invitrogen™ (65-0865-14), BD Pharmnigen™ (553786), BD Pharmnigen™ (553066), BD Pharmnigen™ (552850), Invitrogen™ (MF48020), BioLegend® (141717), Invitrogen™ (48-0862-82)
<i>Fixable Viability Dye eFluor™ 780</i> , CD45R Alexa Fluor® 488 (RA3-6B2), CD138 PE (281-2), CD19 PerCP Cy5.5 (1D3), CD11c APC (N418)	Invitrogen™ (65-0865-14), BD Pharmnigen™ (557669), BD Pharmnigen™ (561070), BD Pharmnigen™ (551001), BioLegend® (117310)
<i>Fixable Viability Dye eFluor™ 780</i> , FITC Rat Anti-Mouse T- and B-cell Activation Antigen (GL7), CD95 PE (Jo2), CD45R APC (RA3-6B2)	Invitrogen™ (65-0865-14), BD Pharmnigen™ (553666), BD Pharmnigen™ (554258), BD Pharmnigen™ (553092)
<i>Fixable Viability Dye eFluor™ 780</i> , CD3 FITC (17A2), CD3 FITC (17A2), ICOS APC (C398.4A), CD4 PE Cy7 (RM4-5)	Invitrogen™ (65-0865-14), BD Pharmnigen™ (555274), eBioscience (17-9949-82), BD Pharmnigen™ (552775)
<i>Fixable Viability Dye eFluor™ 780</i> , Ly6G Alexa Fluor® 700 (1A8), CD45R Alexa Fluor® 488 (RA3-6B2), CD11b PE (M1/70), CD11c PE-Cy7 (HL3), Ly6C BV510 (HK1.4), MHC Class II APC (M5/114.15.2)	Invitrogen™ (65-0865-14), BioLegend (127622), BD Pharmnigen™ (557669), BD Pharmnigen™ (561689), BD Pharmnigen™ (558079), BioLegend® (128033), eBioscience (17-5321-82)

Uni340FP-ACTCCTACGGGAGGCAGCAGT,  
Eubact Uni514RP – ATTACCGCGGCTGCTGGC.  
Relative gene expression for SFB was normalized to total Eubacteria.

### Flow cytometry

Immune cells from mesenteric lymph nodes or spleen were isolated by dissociating the organ on 100 µm strainer using a plunger of a 1 mL syringe. Approximately  $1 \times 10^6$  cells were resuspended in buffer composed of PBS, 0.5% BSA, and 2% FBS. The cells were then resuspended in Fc Block. After 15 min at room temperature, cells were then stained with the following antibodies in Table 1 diluted in FACS buffer according to manufacturer's instructions for 30 min at 4°C in the dark. Cells were then centrifuged and rinsed with FACS buffer, then resuspended with 2% paraformaldehyde for 15 min in the dark at room temperature. Data were collected on a BD FACSymphony A5 and analyzed with FlowJo Software (10.8.1).

### RNA isolation and qPCR quantification

RNA was isolated from tissues using FastRNA Pro Green Kit (MP Biomedical, 116045050) according to the manufacturer's instructions. Briefly, all surfaces were sprayed and cleaned with RNase Zap (Thermo Fisher, AM97890). An aliquot of 1000 µL of RNA Pro solution™ was added to 100–300 mg of sample. The solution and the sample were transferred to a tube containing Lysing Matrix D. The tube was then processed in the FastPrep® instrument for 40 seconds at a setting of 6.0. The tube was then centrifuged at 12,000 rcf for 5 minutes at 4°C. The supernatant was transferred to

a new tube and incubated at room temperature for 5 minutes. 300 µL of chloroform was added to the tube and vortexed for 10 seconds. Then the tube was incubated at room temperature for 5 minutes. The tube was then centrifuged at 12,000 rcf for 5 minutes at 4°C. The upper phase was transferred to a new tube and 500 µL of cold 100% ethanol was added. The tube was then incubated at – 20°C for at least 30 minutes. The tube was then centrifuged at 12,000 rcf for 15 minutes at 4°C. The supernatant was discarded, and the pellet was washed with 500 µL of cold 75% ethanol. Supernatant was discarded, and the pellet was left to air dry for 5 minutes at room temperature. The pellet was then resuspended in 50 ~ 100 µL of DEPC H<sub>2</sub>O and incubated at room temperature for 5 minutes. The RNA in the supernatant quantified by analysis of absorbance using a NanoDrop spectrophotometer.

The RNA was then reverse transcribed to cDNA using a TaqMan Reverse Transcription kit according to manufacturer's protocol (Invitrogen, N8080234). qPCR was performed with an Applied Biosciences StepOne Plus Real Time PCR system as described previously.<sup>37</sup> Transcript levels were determined using the  $\Delta C_T$  approach. Primer sequences were listed previously.<sup>67</sup>

### Analysis of anti-dsDNA autoantibodies by ELISA

ELISAs were performed according to a previously published protocol.<sup>69</sup> Briefly, a 96-well plate (Costar, 07-200-33) was coated with 0.01% poly-L-lysine (Sigma, P8920) in PBS and incubated for 1 h at room temperature. Plates were then washed three times with distilled water and dried. Plates were then coated with 2.5 µg/mL of calf thymus

DNA (Invitrogen, 15633–019) in borate buffered saline (BBS) (17.5 g NaCl, 2.5 g H<sub>3</sub>BO<sub>3</sub>, 38.1 g sodium borate in 1 L H<sub>2</sub>O) and incubated at 4°C overnight. The next day, plates are washed three times with BBS and blocked with 200 µL/well of BBT (BBS with 3% bovine serum albumin and 1% Tween 20) for 2 h at room temperature with gentle rocking. After washing five times with BBS, serial dilutions of control serum and sample sera were incubated on the plate overnight at 4°C. Next, plates were washed three to five times with BBS, and biotinylated goat anti-mouse IgG (Jackson ImmunoRes, 115-065-071) was added. Samples were incubated at room temperature for 2 h with gentle rocking. Avidin-alkaline phosphate conjugate (Sigma, A7294) was added. After 2 h at room temperature, plates were washed five times with BBS, and then 4-nitrophenyl phosphate disodium salt hexahydrate (Sigma-Aldrich, N2765) was added to the plate at 1 mg/mL. Plates were incubated at 37°C protected from light for at least 3 h. Optical densities at 650 nm and 405 nm were determined using a Molecular Devices Microplate reader. Positive control sera were taken from B6.NZM Sle1/Sle2/Sle3 lupus-prone mice with high levels of autoantibodies and used at a dilution of 1:250 in BBT.

### Joint inflammation analysis

Histopathological analyses were done at the Histopathology core at Fox Chase Cancer Center. Murine knee joints were extracted and fixed in phosphate-buffered formalin. For decalcification, samples were incubated in formic acid for 3 days and then embedded in paraffin. Sections of 5 µm of the tissue were stained with hematoxylin and eosin. The fixed and stained sections were blinded and evaluated by an experienced veterinary pathologist according to the criteria previously described [70].

### Statistical analyses

Data were analyzed using Prism software (GraphPad). One-way or two-way ANOVA as well as Mann-Whitney tests were used when appropriate. Error was determined by standard error of the mean. *P* values of < 0.05 were considered significant and were noted as such on figures.

### Acknowledgments

We would like to thank Dr. Roberto Caricchio, Dr. Marc Monestier and Dr. Bettina Buttarò for constructive discussions regarding the study.

### Disclosure statement

No potential conflict of interest was reported by the author(s).

### Funding

C.T. is supported by NIH grants AI153325, AI151893, and AI148770. VT was supported by NIH grant AI168550. The work of A. J. P. K. was supported by the Histopathology Facility under NIH grant P30CA06927.

### Data availability statement

All data are fully available without restriction.

### Ethics statement

All animal experiments were performed in a BSL2 facility under protocols approved by AALAC-accredited Temple University Lewis Katz School of Medicine, Institutional Animal Care and Use Committee (IACUC #4868) in accordance with guidelines set forth by the USDA and PHS Policy on Humane Care and Use of Laboratory Animal Welfare. The institution has an Animal Welfare Assurance on file with the NIH Office for the Protection of Research Risks, Number A3594–01.

### References

1. Schnabel J. Protein folding: the dark side of proteins. *Nature*. 2010;464(7290):828–829. doi:10.1038/464828a.
2. Ross CA, Poirier MA. Protein aggregation and neurodegenerative disease. *Nat Med*. 2004;10(Suppl):S10–7. doi:10.1038/nm1066.
3. Hull RL, Rebecca L, Westermarck, GT, Westermarck, P and Kahn, SE. Islet amyloid: a critical entity in the pathogenesis of type 2 diabetes. *J Clin Endocrinol Metab*. 2004;89(8):3629–3643. doi:10.1210/jc.2004-0405.
4. Cherny I, Rockah, L, Levy-Nissenbaum, O, Gophna, Uri, Ron, EZ, Gazit, E. The formation of *Escherichia coli* curli amyloid fibrils is mediated by prion-like peptide repeats. *J Mol Biol*. 2005;352(2):245–252. doi:10.1016/j.jmb.2005.07.028.
5. Barnhart MM, Chapman MR. Curli biogenesis and function. *Annu Rev Microbiol*. 2006;60(1):131–147. doi:10.1146/annurev.micro.60.080805.142106.
6. Chapman MR, Robinson, LS, Pinkner, JS, Roth, R Heuser, J Hammar, M Normark, S Hultgren, SJ. Role

- of *Escherichia coli* curli operons in directing amyloid fiber formation. *Science*. 2002;295(5556):851–855. doi:10.1126/science.1067484.
7. Hufnagel DA, Tukul C, Chapman MR, True HL, True HL. Disease to dirt: the biology of microbial amyloids. *PLoS Pathog*. 2013;9(11):e1003740. doi:10.1371/journal.ppat.1003740.
  8. Tursi S, Puligedda RD, Szabo P, Nicastro LK, Miller AL, Qiu C, Gallucci S, Relkin NR, Buttaro BA, Dessain SK, et al. Salmonella Typhimurium biofilm disruption by a human antibody that binds a pan-amyloid epitope on curli. *Nat Commun*. 2020;11(1). doi:10.1038/s41467-020-14685-3.
  9. Tursi SA, Tukul C. Curli-containing enteric biofilms inside and out: matrix composition, immune recognition, and disease implications. *Microbiol Mol Biol Rev*. 2018;82(4). doi:10.1128/MMBR.00028-18.
  10. White AP, Gibson, DL, Kim, W, Kay, WW, Surette, MG. Thin aggregative fimbriae and cellulose enhance long-term survival and persistence of *Salmonella*. *J Bacteriol*. 2006;188(9):3219–3227. doi:10.1128/JB.188.9.3219-3227.2006.
  11. Vidakovic L, Singh PK, Hartmann R, Nadell CD, Drescher K. Dynamic biofilm architecture confers individual and collective mechanisms of viral protection. *Nat Microbiol*. 2018;3(1):26–31. doi:10.1038/s41564-017-0050-1.
  12. McCrate OA, Zhou, X, Reichhardt, C, Cegelski, L. Sum of the parts: composition and architecture of the bacterial extracellular matrix. *J Mol Biol*. 2013;425(22):4286–4294. doi:10.1016/j.jmb.2013.06.022.
  13. Tukul C, Raffatellu M, Humphries AD, Wilson RP, Andrews-Polymenis HL, Gull T, Figueiredo JF, Wong MH, Michelsen KS, Akçelik M, et al. CsgA is a pathogen-associated molecular pattern of *Salmonella enterica* serotype typhimurium that is recognized by Toll-like receptor 2. *Mol Microbiol*. 2005;58(1):289–304. doi:10.1111/j.1365-2958.2005.04825.x.
  14. Hoshino K, Takeuchi, O, Kawai, T, Sanjo, H, Ogawa, T, Takeda, Y, Takeda, K Akira, S. Cutting edge: toll-like receptor 4 (TLR4)-deficient mice are hyporesponsive to lipopolysaccharide: evidence for TLR4 as the Lps gene product. *J Immunol*. 1999;162(7):3749–3752. doi:10.4049/jimmunol.162.7.3749.
  15. Gewirtz AT, Navas, TA, Lyons, S, Godowski, PJ, Madara, JL. Cutting edge: bacterial flagellin activates basolaterally expressed TLR5 to induce epithelial proinflammatory gene expression. *J Immunol*. 2001;167(4):1882–1885. doi:10.4049/jimmunol.167.4.1882.
  16. Franchi L, Amer A, Body-Malapel M, Kanneganti T-D, Özören N, Jagirdar R, Inohara N, Vandenabeele P, Bertin J, Coyle A, et al. Cytosolic flagellin requires Ipaf for activation of caspase-1 and interleukin 1 $\beta$  in salmonella-infected macrophages. *Nat Immunol*. 2006;7(6):576–582. doi:10.1038/ni1346.
  17. Miao EA, Alpuche-Aranda CM, Dors M, Clark AE, Bader MW, Miller SI, Aderem A. Cytoplasmic flagellin activates caspase-1 and secretion of interleukin 1 $\beta$  via Ipaf. *Nat Immunol*. 2006;7(6):569–575. doi:10.1038/ni1344.
  18. Miller AL, Nicastro, LK, Bessho, S, Grando, K, White, AP, Zhang, Yi, Queisser, G, Buttaro, BA, Tukul, C. Nitrate is an Environmental Cue in the Gut for *Salmonella enterica* Serovar Typhimurium Biofilm Dispersal through Curli Repression and Flagellum Activation via Cyclic-di-GMP Signaling. *mBio*. 2022;13(1):e0288621. doi:10.1128/mbio.02886-21.
  19. Tukul C, Nishimori JH, Wilson RP, Winter MG, Keestra AM, Van Putten JPM, Bäumlér AJ. Toll-like receptors 1 and 2 cooperatively mediate immune responses to curli, a common amyloid from enterobacterial biofilms. *Cell Microbiol*. 2010;12(10):1495–1505. doi:10.1111/j.1462-5822.2010.01485.x.
  20. Rapsinski GJ, Wynosky-Dolfi, MA, Oppong, GO, Tursi, SA, Wilson, RP, Brodsky, IE, Tukul, C. Toll-Like Receptor 2 and NLRP3 Cooperate to Recognize a Functional Bacterial Amyloid, Curli. *Infect Immun*. 2015;83(2):693–701. doi:10.1128/IAI.02370-14.
  21. Tukul C, Wilson RP, Nishimori JH, Pezeshki M, Chromy BA, Bäumlér AJ. Responses to amyloids of microbial and host origin are mediated through Toll-like receptor 2. *Cell Host & Microbe*. 2009;6(1):45–53. doi:10.1016/j.chom.2009.05.020.
  22. Tursi SA, Lee, EY, Medeiros, NJ, Lee, MH, Nicastro, LK, Buttaro, B, Gallucci, S, Wilson, RP, Wong, GCL, Tukul, C. Bacterial amyloid curli acts as a carrier for DNA to elicit an autoimmune response via TLR2 and TLR9. *PLoS Pathog*. 2017;13(4):e1006315. doi:10.1371/journal.ppat.1006315.
  23. Gallo PM, Rapsinski, GJ, Wilson, RP, Oppong, GO, Sriram, U, Goulían, M, Buttaro, B, Caricchio, R, Gallucci, S, Tukul, C. Amyloid-DNA Composites of Bacterial Biofilms Stimulate Autoimmunity. *Immunity*. 2015;42(6):1171–1184. doi:10.1016/j.immuni.2015.06.002.
  24. Nishimori JH, Newman, TN, Oppong, GO, Rapsinski, GJ, Yen, JH, Biesecker, SG, Wilson, RP, Butler, BP, Winter, MG, Tsolis, RM. Microbial amyloids induce interleukin 17A (IL-17A) and IL-22 responses via Toll-like receptor 2 activation in the intestinal mucosa. *Infect Immun*. 2012;80(12):4398–4408. doi:10.1128/IAI.00911-12.
  25. Miller AL. Microbiome or Infections: amyloid-Containing Biofilms as a Trigger for Complex Human Diseases. *Front Immunol*. 2021;12:638867. doi:10.3389/fimmu.2021.638867.
  26. Sampson TR, Challis C, Jain N, Moiseyenko A, Ladinsky MS, Shastri GG, Thron T, Needham BD, Horvath I, Debelius JW, et al. A gut bacterial amyloid promotes  $\alpha$ -synuclein aggregation and motor impairment in mice. *Elife*. 2020;9:9. doi:10.7554/eLife.53111.
  27. Chen SG, Stribinskis V, Rane MJ, Demuth DR, Gozal E, Roberts AM, Jagadapillai R, Liu R, Choe K, Shivakumar B, et al. Exposure to the functional

- bacterial amyloid protein curli enhances alpha-synuclein aggregation in aged Fischer 344 rats and *Caenorhabditis elegans*. *Sci Rep*. 2016;6(1):34477. doi:10.1038/srep34477.
28. Friedland RP, Chapman MR, Bliska JB. The role of microbial amyloid in neurodegeneration. *PLoS Pathog*. 2017;13(12):e1006654. doi:10.1371/journal.ppat.1006654.
  29. Nicastro L, Tükel C. Bacterial amyloids: the link between bacterial infections and autoimmunity. *Trends Microbiol*. 2019;27(11):954–963. doi:10.1016/j.tim.2019.07.002.
  30. Miller AL, Pasternak JA, Medeiros NJ, Nicastro LK, Tursi SA, Hansen EG, Krochak R, Sokaribo AS, MacKenzie KD, Palmer MB, et al. In vivo synthesis of bacterial amyloid curli contributes to joint inflammation during *S. Typhimurium* Infection. *PLoS Pathog*. 2020;16(7):e1008591. doi:10.1371/journal.ppat.1008591.
  31. Pachucki RJ, Corradetti C, Kohler L, Ghadiali J, Gallo PM, Nicastro L, Tursi SA, Gallucci S, Tükel Ç, Caricchio R. Persistent bacteriuria and antibodies recognizing curli/eDNA complexes from *Escherichia coli* are linked to flares in systemic lupus erythematosus. *Arthritis Rheumatol*. 2020;72(11):1872–1881. doi:10.1002/art.41400.
  32. Candelli M, Franza L, Pignataro G, Ojetti V, Covino M, Piccioni A, Gasbarrini A, Franceschi F. Interaction between lipopolysaccharide and gut microbiota in inflammatory bowel diseases. *IJMS*. 2021;22(12):6242. doi:10.3390/ijms22126242.
  33. Tran HQ, Ley RE, Gewirtz AT, Chassaing B. Flagellin-elicited adaptive immunity suppresses flagellated microbiota and vaccinates against chronic inflammatory diseases. *Nat Commun*. 2019;10(1):5650. doi:10.1038/s41467-019-13538-y.
  34. Lohr J, Knoechel B, Wang JJ, Villarino AV, Abbas AK. Role of IL-17 and regulatory T lymphocytes in a systemic autoimmune disease. *J Exp Med*. 2006;203(13):2785–2791. doi:10.1084/jem.20061341.
  35. Ivanov II, Atarashi K, Manel N, Brodie EL, Shima T, Karaoz U, Wei D, Goldfarb KC, Santee CA, Lynch SV, et al. Induction of intestinal Th17 cells by segmented filamentous bacteria. *Cell*. 2009;139(3):485–498. doi:10.1016/j.cell.2009.09.033.
  36. Nicastro LK, Tursi SA, Le LS, Miller AL, Efimov A, Buttaro B, Tam V, Tükel Ç. Cytotoxic curli intermediates form during salmonella biofilm development. *J Bacteriol*. 2019;201(18). doi:10.1128/JB.00095-19.
  37. Nicastro LK, de Anda J, Jain N, Grando KCM, Miller AL, Bessho S, Gallucci S, Wong GCL, Tükel C. Assembly of ordered DNA-curli fibril complexes during *Salmonella* biofilm formation correlates with strengths of the type I interferon and autoimmune responses. *PLoS Pathog*. 2022;18(8):e1010742. doi:10.1371/journal.ppat.1010742.
  38. Pan M, Kang I, Craft J, Yin Z. Resistance to development of collagen-induced arthritis in C57BL/6 mice is due to a defect in secondary, but not in primary, immune response. *J Clin Immunol*. 2004;24(5):481–491. doi:10.1023/B:JOCL.0000040919.16739.44.
  39. Macfarlane S, Bahrami B, Macfarlane GT. Mucosal biofilm communities in the human intestinal tract. *Adv Appl Microbiol*. 2011;75:111–143.
  40. Lu H, Que Y, Wu X, Guan T, Guo H. Metabolomics deciphered metabolic reprogramming required for biofilm formation. *Sci Rep*. 2019;9(1):13160. doi:10.1038/s41598-019-49603-1.
  41. Hathroubi S, Mekni MA, Domenico P, Nguyen D, Jacques M. Biofilms: microbial shelters against antibiotics. *Microb Drug Resist*. 2017;23(2):147–156. doi:10.1089/mdr.2016.0087.
  42. Hoiby N. A short history of microbial biofilms and biofilm infections. *APMIS*. 2017;125(4):272–275. doi:10.1111/apm.12686.
  43. Koo H, Allan RN, Howlin RP, Stoodley P, Hall-Stoodley L. Targeting microbial biofilms: current and prospective therapeutic strategies. *Nat Rev Microbiol*. 2017;15(12):740–755. doi:10.1038/nrmicro.2017.99.
  44. Tamayo R, Patimalla B, Camilli A. Growth in a biofilm induces a hyperinfectious phenotype in *Vibrio cholerae*. *Infect Immun*. 2010;78(8):3560–3569. doi:10.1128/IAI.00048-10.
  45. Gallego-Hernandez AL, DePas WH, Park JH, Teschler JK, Hartmann R, Jeckel H, Drescher K, Beyhan S, Newman DK, Yildiz FH, et al. Upregulation of virulence genes promotes *Vibrio cholerae* biofilm hyperinfectivity. *Proc Natl Acad Sci USA*. 2020;117(20):11010–11017. doi:10.1073/pnas.1916571117.
  46. Di Domizio J, Zhang R, Staggs LJ, Gagea M, Zhuo M, Ladbury JE, Cao W. Binding with nucleic acids or glycosaminoglycans converts soluble protein oligomers to amyloid. *J Biol Chem*. 2012;287(1):736–747. doi:10.1074/jbc.M111.238477.
  47. Jimenez JS. Protein-DNA interaction at the origin of neurological diseases: a hypothesis. *J Alzheimers Dis*. 2010;22(2):375–391. doi:10.3233/JAD-2010-100189.
  48. Maloney B, Lahiri DK. The Alzheimer's amyloid beta-peptide (Aβ) binds a specific DNA Aβ-interacting domain (AβID) in the APP, BACE1, and APOE promoters in a sequence-specific manner: characterizing a new regulatory motif. *Gene*. 2011;488(1–2):1–12. doi:10.1016/j.gene.2011.06.004.
  49. Grando K, Nicastro LK, Tursi SA, De Anda J, Lee EY, Wong GCL, Tükel Ç. Phenol-soluble modulins from staphylococcus aureus biofilms form complexes with DNA to drive autoimmunity. *Front Cell Infect Microbiol*. 2022;12. doi:10.3389/fcimb.2022.884065.
  50. Oppong GO. Epithelial cells augment barrier function via activation of the toll-like receptor 2/phosphatidylinositol 3-kinase pathway upon recognition of salmonella enterica serovar typhimurium curli fibrils in the gut. *Infect Immun*. 2013;81(2):478–486. doi:10.1128/IAI.00453-12.
  51. Alduraibi FK, Sullivan KA, Chatham WW, Hsu HC, Mountz JD. Interrelation of T cell cytokines and



- autoantibodies in systemic lupus erythematosus: a cross-sectional study. *Clin Immunol.* **2023**;247:109239. doi:10.1016/j.clim.2023.109239.
52. Chaurasia S, Shasany AK, Aggarwal A, Misra R. Recombinant *Salmonella typhimurium* outer membrane protein a is recognized by synovial fluid CD8 cells and stimulates synovial fluid mononuclear cells to produce interleukin (IL)-17/IL-23 in patients with reactive arthritis and undifferentiated spondyloarthropathy. *Clin Exp Immunol.* **2016**;185(2):210–218. doi:10.1111/cei.12799.
  53. Terui H, Yamasaki K, Wada-Irimada M, Onodera-Amagai M, Hatchome N, Mizuashi M, Yamashita R, Kawabe T, Ishii N, Abe T, et al. *Staphylococcus aureus* skin colonization promotes SLE-like autoimmune inflammation via neutrophil activation and the IL-23/IL-17 axis. *Sci Immunol.* **2022**;7(76):eabm9811. doi:10.1126/sciimmunol.abm9811.
  54. Vijay-Kumar M, Aitken JD, Carvalho FA, Cullender TC, Mwangi S, Srinivasan S, Sitaraman SV, Knight R, Ley RE, Gewirtz AT, et al. Metabolic syndrome and altered gut microbiota in mice lacking Toll-like receptor 5. *Science.* **2010**;328(5975):228–231. doi:10.1126/science.1179721.
  55. Alpizar-Rodriguez D, Lesker TR, Gronow A, Gilbert B, Raemy E, Lamacchia C, Gabay C, Finckh A, Strowig T. *Prevotella copri* in individuals at risk for rheumatoid arthritis. *Ann Rheum Dis.* **2019**;78(5):590–593. doi:10.1136/annrheumdis-2018-214514.
  56. Azzouz D, Omarbekova A, Heguy A, Schwudke D, Gisch N, Rovin BH, Caricchio R, Buyon JP, Alekseyenko AV, Silverman GJ, et al. Lupus nephritis is linked to disease-activity associated expansions and immunity to a gut commensal. *Ann Rheum Dis.* **2019**;78(7):947–956. doi:10.1136/annrheumdis-2018-214856.
  57. Ishigame H, Kakuta S, Nagai T, Kadoki M, Nambu A, Komiyama Y, Fujikado N, Tanahashi Y, Akitsu A, Kotaki H, et al. Differential roles of interleukin-17A and -17F in host defense against mucosal bacterial infection and allergic responses. *Immunity.* **2009**;30(1):108–119. doi:10.1016/j.immuni.2008.11.009.
  58. Lawrence AE, Berger RP, Hill DR, Huang S, Yadagiri VK, Bons B, Fields C, Sule GJ, Knight JS, Wobus CE, et al. Human neutrophil IL1 $\beta$  directs intestinal epithelial cell extrusion during *Salmonella* infection. *PLoS Pathog.* **2022**;18(10):e1010855. doi:10.1371/journal.ppat.1010855.
  59. Migliorini P, Italiani P, Pratesi F, Puxeddu I, Boraschi D. The IL-1 family cytokines and receptors in autoimmune diseases. *Autoimmun Rev.* **2020**;19(9):102617. doi:10.1016/j.autrev.2020.102617.
  60. Shlomchik MJ, Weisel F. Germinal center selection and the development of memory B and plasma cells. *Immunol Rev.* **2012**;247(1):52–63. doi:10.1111/j.1600-065X.2012.01124.x.
  61. Herlands RA, William J, Hershberg U, Shlomchik MJ. Anti-chromatin antibodies drive in vivo antigen-specific activation and somatic hypermutation of rheumatoid factor B cells at extrafollicular sites. *Eur J Immunol.* **2007**;37(12):3339–3351. doi:10.1002/eji.200737752.
  62. Sang A, Niu H, Cullen J, Choi SC, Zheng YY, Wang H, Shlomchik MJ, Morel L. Activation of rheumatoid factor-specific B cells is antigen dependent and occurs preferentially outside of germinal centers in the lupus-prone NZM2410 mouse model. *J Immunol.* **2014**;193(4):1609–1621. doi:10.4049/jimmunol.1303000.
  63. Di Niro R, Lee SJ, Vander Heiden JA, Elsner RA, Trivedi N, Bannock JM, Gupta NT, Kleinstein SH, Vigneault F, Gilbert TJ, et al. *Salmonella* infection drives promiscuous B cell activation followed by extrafollicular affinity maturation. *Immunity.* **2015**;43(1):120–131. doi:10.1016/j.immuni.2015.06.013.
  64. Larsen P, Nielsen, JL, Dueholm, MS, Wetzel, R, Otzen, D, Nielsen, PH. Amyloid adhesins are abundant in natural biofilms. *Environ Microbiol.* **2007**;9(12):3077–3090. doi:10.1111/j.1462-2920.2007.01418.x.
  65. Lim JY, May JM, Cegelski L. Dimethyl sulfoxide and ethanol elicit increased amyloid biogenesis and amyloid-integrated biofilm formation in *Escherichia coli*. *Appl Environ Microbiol.* **2012**;78(9):3369–3378. doi:10.1128/AEM.07743-11.
  66. Zhu W, Winter MG, Byndloss MX, Spiga L, Duerkop BA, Hughes ER, Büttner L, de Lima Romão E, Behrendt CL, Lopez CA, et al. Precision editing of the gut microbiota ameliorates colitis. *Nature.* **2018**;553(7687):208–211. doi:10.1038/nature25172.
  67. Wilson RP, Tursi SA, Rapsinski GJ, Medeiros NJ, Le LS, Kotredes KP, Patel S, Liverani E, Sun S, Zhu W, et al. STAT2 dependent Type I interferon response promotes dysbiosis and luminal expansion of the enteric pathogen *Salmonella typhimurium*. *PLoS Pathog.* **2019**;15(4):e1007745. doi:10.1371/journal.ppat.1007745.
  68. Kumar P, Monin L, Castillo P, Elsegeiny W, Horne W, Eddens T, Vikram A, Good M, Schoenborn AA, Bibby K, et al. (2016). Intestinal Interleukin-17 Receptor Signaling Mediates Reciprocal Control of the Gut Microbiota and Autoimmune Inflammation. *Immunity*, 44(3), 659–671. doi:10.1016/j.immuni.2016.02.007.
  69. Sriram U, Varghese, L, Bennett, HL, Jog, NR, Shivers, DK, Ning, Yue, Behrens, EM, Caricchio, R, Gallucci, S. Myeloid dendritic cells from B6.NZM Sle1/Sle2/Sle3 lupus-prone mice express an IFN signature that precedes disease onset. *J Immunol.* **2012**;189(1):80–91. doi:10.4049/jimmunol.1101686.
  70. Noto Llana M, Sarnacki, SH, Vazquez, MV, Gartner, AS, Giacomodonato, MN, Cerquetti, MC. *Salmonella enterica* induces joint inflammation and expression of interleukin-17 in draining lymph nodes early after onset of enterocolitis in mice. *Infect Immun.* **2012**;80(6):2231–2239. doi:10.1128/IAI.00324-12.